Colloquium: Understanding ion motion in disordered solids from impedance spectroscopy scaling

D. L. Sidebottom

Department of Physics, Creighton University, 2500 California Plaza, Omaha, Nebraska 68178, USA

(Published 6 July 2009)

ac impedance measurements of ion-conducting glasses provide considerable insight into the nature of the ionic motions in disordered solids. However, interpreting the ac impedance has been a matter of considerable debate, particularly in regards to how best to represent the relaxation process that is the result of a transition from correlated to uncorrelated ion hopping. Although interpretations based upon the electric modulus have featured prominently in the earlier literature, direct analysis of the complex conductivity in the frequency domain is gaining popularity as it provides direct (via Fourier transform) information regarding the microscopic mean-squared displacement of ions. Here many recent findings are summarized that emphasize the scaling features present in the impedance spectra to demonstrate how the casual researcher might interpret ac impedance results without elaborate curve fitting.

DOI: 10.1103/RevModPhys.81.999 PACS number(s): 66.30.H−, 61.43.Fs, 66.10.Ed, 66.30.Dn

CONTENTS

I. INTRODUCTION

Most students are familiar with the major advances in understanding electron conduction in crystals as are conveyed in a typical course on *Solid State Physics* (Kittel, 2005). There one finds that the crystal structure is key to the various electron conduction phenomena in both metals and semiconductors. But, of course, not all solids are crystalline and not all conductors are electronic. There are many disordered solids such as polymers and oxide glasses wherein the conduction of mobile ions is of considerable interest. Today, interest in the dynamics in disordered materials is driven by the multitude of novel applications these materials find in such devices as high-energy, environmentally safe batteries and electronic sensors. So profound is the interest in devices based upon ion transport in both ordered and disordered materials that this expanding field of research has come to be known as *solid-state ionics* (Kudo and Fueki, 1990).

Like solid-state physicists, those working in the solid-state ionics field are keen to understand the conduction phenomena, not of electrons in crystals but of ions in a disordered (nonperiodic) host matrix. We begin by comparing and contrasting the conduction of electrons in a metal to that of ions in a glass. In a metal, the matrix is comprised of an ordered three-dimensional (3D) array of ion cores whose excess valence electrons have dissociated to form a continuous sea of reasonably free electrons. This sea of electrons provides the electrostatic "glue" that maintains the crystal structure. Because the electron has a small mass, its de Broglie wavelength is rather large and quantum-mechanical considerations become noticeable in its movement within the matrix. Indeed much of the conduction phenomena in metals and semiconductors result from diffraction of the electron wave from the periodic lattice of ion cores.

In ion-conducting polymers and oxide glasses, the 3D matrix is nonperiodic and generally held together by stronger covalent bonds. As many are aware, glasses typically shatter on impact while metals just become dented. In many disordered ion conductors, the valence electrons are completely taken up in the formation of the covalent bonds that form the matrix, and no excess is available for electronic conduction. Instead, mobile ions are introduced into the disordered matrix by various chemical additions. Often salts are added to a polymer matrix and become dissociated into cation and anion pairs that can diffuse about. In oxide glasses, the addition of an alkali oxide (like Li_2O added to SiO_2) often ruptures a bridging oxygen connection between two Si resulting in two nonbridging oxygens with negative charge to which two Li cations are ionically bonded. This is shown in Fig. 1. Here the ions are far more mas-

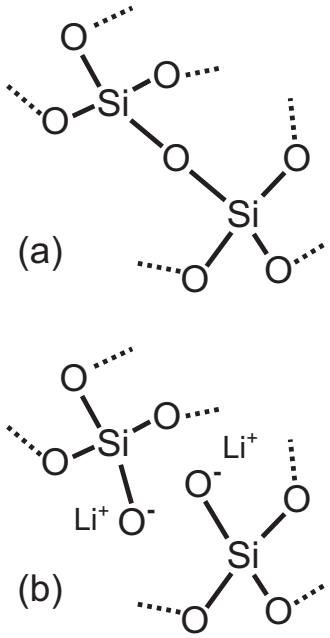

FIG. 1. Covalent network of pure SiO_2. (b) Formation of nonbridging oxygen sites on addition of Li_2O.

sive than the electron, and quantum-mechanical considerations are far less relevant to discussion of how these ions move about.

II. BASIC CONCEPTS

Although there are a variety of ion-conducting solids, we take as an example the lithium silicate glass presented in Fig. 1, whose key elements are much the same: the system consists of a rigid, disordered matrix through which the ions travel together with charge-compensating sites [in this case, the nonbridging oxygens (NBOs)] fixed to the matrix about which the ions are loosely tethered by weaker-than-covalent ionic bonds. Because of the weakness of these ionic bonds, often thermal energy in the solid can provide the energy needed for the ion to dissociate from its site. An additional energy (strain energy) is needed for the ion to squeeze through passageways in the matrix (Anderson and Stuart, 1954) in order to "hop" to an adjacent site. Together these two energies form a so-called activation energy, the energy associated with the hop of an ion between adjacent sites. The rate of hopping is then controlled by the temperature and for most materials is given by the Boltzmann factor (or Arrhenius law) $f_H = \Omega \exp(-E/kT)$.

A typical ion-conducting solid contains some 10^{22} ions per cubic centimeter. Because the charge-compensating sites are more or less randomly positioned in the matrix, they should have an average separation $\xi \approx N^{-1/3}$, where N is the number density of ions. So for $N \approx 10^{22}$ cm^{-3}, the average ion separation is $\xi \approx 5$ Å. Molecular-dynamics simulations may be able to track the position of some of these over time, but otherwise we may need to satisfy ourselves with ensemble-averaged quantities such as the mean-squared displacement $\langle r^2(t) \rangle$, a key quantity of interest in many theoretical approaches (Scher and Lax, 1973a, 1973b; Funke, 1993; Funke and Wilmer, 1999), to describe the motion.

III. OBSERVING ION MOTION BY IMPEDANCE SPECTROSCOPY

There are many techniques that indirectly probe the motion of ions in the solid. But here we restrict our attention to ac impedance techniques that track ion motion through the electrical response of the material resulting from the movement of mobile ions. Suppose we form our solid sample into a thin disk of thickness d and apply two metallic electrodes of area A onto the opposite faces. The two electrodes form a parallel-plate capacitor with the sample as an unknown dielectric filling (Jain, 1993; ASTM designation, 1995). Without the filling, the empty capacitance is given by $C = \varepsilon_0 A/d$. If we connect a source of alternating current, we form a parallel RC circuit where both the resistance $R(\omega)$ and capacitance $C(\omega)$ are frequency dependent due to the time-dependent motion of the ions as well as other atoms in the material. Ohm's law allows the current and voltage measured in our circuit to be reduced to a complex impedance $Z*(\omega)$, whose inverse is given by (Tipler, 1999)

$$[Z^*(\omega)]^{-1} = [1/R(\omega)] - i[\omega C(\omega)] = \frac{A}{d}\{\sigma(\omega) - i\omega\varepsilon_0\varepsilon(\omega)\}. \quad (1)$$

The geometry of the electrodes (A/d) can be factored out to obtain the conductivity $\sigma(\omega)$ and dielectric constant $\varepsilon(\omega)$ inherent in the material itself. These can be thought of as real and imaginary parts of a complex conductivity $\sigma^*(\omega)$ and permittivity $\varepsilon^*(\omega)$,

$$\sigma^*(\omega) = \sigma(\omega) + i\omega\varepsilon_0\varepsilon(\omega) = i\omega\varepsilon_0\varepsilon^*(\omega) = i\omega\varepsilon_0[\varepsilon(\omega) - i\varepsilon''(\omega)]. \quad (2)$$

But what insight does $\sigma^*(\omega)$ provide with regard to the ion motions? The answer lies in linear-response theory (Kubo, 1957; Sidebottom *et al.*, 2000; Roling *et al.*, 2001) where the contribution of ion motions to the frequency-dependent conductivity arising from ion motions is given by a Fourier transform of the mean-squared displacement (Roling *et al.*, 2001),

$$\sigma^*_{\text{ion}}(\omega) = -\omega^2 \frac{Nq^2}{6kT} \lim_{\delta \to +0} \int_0^\infty \langle r^2(t) \rangle \exp(-i\omega t - \delta t) dt. \quad (3)$$

This relationship provides the important bridge between experimental impedance measurements and the theoretical description of microscopic ion motions. In principle [and even in practice (Roling, 1999; Roling *et al.*, 2001)], this expression can be inverted to obtain the time-dependent mean-squared displacement of mobile ions directly from measurements of the ac conductivity. But even more importantly, the relation implies that the

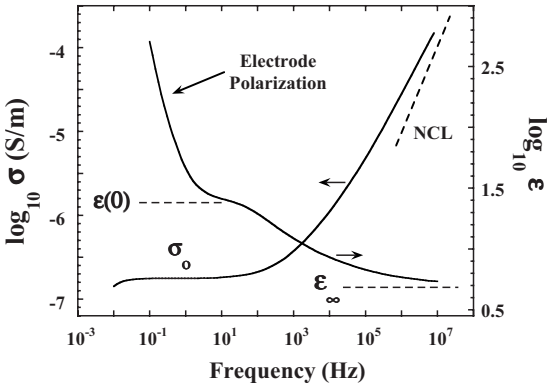

FIG. 2. Schematic representation of how the ac conductivity and dielectric constant typically depend upon frequency for an ionic material. Several of the limiting features are labeled.

frequency-dependent properties of $\sigma^*_{\text{ion}}(\omega)$ are directly related (via Fourier analysis) to time-dependent motions of the ions.

Now we consider some experimental data. What one typically observes for ion-conducting glasses like our lithium silicate is a frequency-dependent conductivity and dielectric constant like that shown in Fig. 2. Here we see a considerable dependence of both quantities on the frequency of the applied electric field. Starting at low frequencies, we find a large increase with decreasing frequency of the dielectric constant which, in the limit of a dc field, attains a plateau value. This phenomenon results from the presence of metallic, or so-called blocking electrodes, that do not permit transfer of mobile ions into the external measuring circuit. As a result, the ions "pile up" near one electrode leaving a depletion layer near the opposite electrode that produces a drop off of the conduction and a large bulk polarization of the specimen. Although this "electrode polarization" (Macedo *et al.*, 1972) is a direct result of the ion motion, it is a nonequilibrium, extrinsic feature that depends both upon the nature of the electrode interface and the thickness of the specimen (Hyde *et al.*, 1987).

As we move to higher frequencies, we observe a short plateau in the conductivity σ_0. In terms of the mean-squared displacement, this so-called dc conductivity represents the long-range diffusion of ions as they hop from site to site through the matrix. In the dielectric constant, we observe a shoulder that suggests an incipient polarization occurring in this same frequency range. We can understand this polarization to be associated with the growth and shrinkage of a dipole moment with a maximum magnitude $p \approx q\xi/2$ that occurs during the hop. This growth and shrinkage is in many respects similar to the rotational relaxation that occurs for a collection of noninteracting permanent dipoles of dipole moment p for which (Jonscher, 1983)

$$\Delta\varepsilon = \frac{Np^2}{3\varepsilon_0 kT}, \tag{4}$$

where N is the density of dipoles, k is the Boltzmann constant ($k = 1.38 \times 10^{-23}$ J/K), and T is the temperature. Making this analogy, we can estimate (Sidebottom, 1999a) a size for the stepwise increase in $\varepsilon(\omega)$ due to an ion hop to be

$$\Delta\varepsilon = \frac{Nq^2\xi^2}{12\varepsilon_0 kT}. \tag{5}$$

For a typical alkali oxide glass with $N \approx 10^{28}$ m^{-3}, the increase in dielectric constant is $\Delta\varepsilon \approx 10$ and at room temperature one obtains from Eq. (5) a value of $\xi \approx 1.3$ Å, which is comparable to the mean spacing between the charge-compensating sites.

As we move still further up in frequency, we see in Fig. 2 a dramatic increase in $\sigma(\omega)$ and a leveling off in $\varepsilon(\omega)$. The leveling off of the dielectric constant occurs because, in addition to the mean-squared displacement of mobile ions, our matrix contains atoms that have become elastically polarized under the influence of the applied field. These atomic and electronic polarizations occur at frequencies well above 1 GHz (Jonscher, 1983) leaving behind a plateau ε_∞, atop which the contribution due to (nonelastic) ion motion rests.

The conductivity increases with increasing frequency in a roughly power-law manner, and in the high-frequency limit the data appear to approach a linear [or superlinear (Cramer *et al.*, 1995)] dependence on frequency. From Eq. (2), the linear frequency dependence would imply a regime where the dielectric loss is frequency independent—a regime often referred to as the "nearly constant loss" (NCL) regime. The NCL is a feature that is currently much debated (Ngai, 1999; Rivera *et al.*, 2002; Murugavel and Roling, 2003; Sidebottom, 2005) and has created much recent research interest.

Putting all this together, we can approximate the frequency dependence of the ac conductivity, aside from the portion affected by electrode polarization (Macdonald, 1994), with the following empirical function:

$$\sigma'(f) \approx \sigma_0[1 + (f/f_0)^n] + Af. \tag{6}$$

This sort of power-law description of the ac conductivity has been advocated by several authors (Jonscher, 1977; Almond and West, 1983a, 1983b; Almond *et al.*, 1983; Elliott, 1994a; Nowick *et al.*, 1998). Values for the exponent n range from 0.5 to 0.7 with a concentration of results near $n = \frac{2}{3}$ (Sidebottom *et al.*, 1995a; Macdonald, 2005). The second, linear, term in the expression represents the NCL. It should be noted that the separation in Eq. (6) of a fractal power law and a linear term is entirely empirical as experimental data generally exhibit a *continuous* increase in the logarithmic slope of the ac conductivity with increasing frequency. Nevertheless, some studies (Sidebottom *et al.*, 1995b; Ngai, 1999) do suggest the NCL regime involves distinctly different kinds of ion movement.

What does this frequency dependence tell us about ion motions? At low frequencies, the dc conductivity implies that the mean-squared displacement is linear,

$$\langle r^2(t)\rangle_{\rm dc} \approx Dt. \tag{7}$$

This linear time dependence is just a reflection of the random diffusion of the ions as they migrate from site to site through the disordered matrix. Such a time-dependent mean-squared displacement is found in the classical random walk model of diffusion and is a hallmark of uncorrelated motions (Gefen *et al.*, 1983). The diffusion coefficient for this walk would be $D=\xi^2/6\tau=\xi^2 f_H/6$, where ξ is the mean hopping distance and $\tau=1/f_H$ is the average time taken to complete a single hop. Applying the Fourier transformation [Eq. (3)] to Eq. (7), one obtains the Nernst-Einstein relationship between the dc conductivity and the hopping rate,

$$\sigma_0 = (Nq^2\xi^2/6kT)f_H. \tag{8}$$

At higher frequencies it follows that the mean-squared displacement becomes nonlinear and must be described (at least for $f \geqslant f_H$) by

$$\langle r^2(t)\rangle_{\rm ac} \approx \xi^2(t/\tau)^{1-n}, \quad t<\tau. \tag{9}$$

In contrast to the dc regime, this sort of mean-squared displacement is subdiffusive and indicates an ion motion that is nonrandom or temporally correlated.

What is the source for this correlated motion? Such a subdiffusive mean-squared displacement is well known in the anomalous diffusion of a random walk limited to a fractal geometry (Gefen *et al.*, 1983). Hence one could envision a fractal network of conducting trails that percolate through the glassy matrix along which ions prefer to travel (Greaves *et al.*, 1991). These trails would appear self-similar over length scales smaller than ξ and $\langle r^2(t)\rangle$ would exhibit a time dependence similar to that in Eq. (9). Motion on length scales greater than ξ would appear uncorrelated and fully diffusive, behaving in accordance with Eq. (7). While this picture of the ion motion could in principle account for the observed ac conductivity (Sidebottom *et al.*, 1995c), and may very well be the correct interpretation for certain conducting materials that possess well-established fractal pathways (Jund *et al.*, 2001), it does not appear to offer the correct interpretation for ac conductivity of the sort of alkali oxide glasses presently discussed. The simple reason is that this anomalous diffusion model—as applied to $\sigma(\omega)$ like that typical of Fig. 2—would necessitate a correlation length of only about 2–5 Å. The existence of a self-similar fractal network operative *inside* this length scale is highly improbable (Sidebottom *et al.*, 1995c). Instead, the correlated motion is better pictured as motion in which the ions perform numerous "unsuccessful" back-and-forth hops (Funke, 1993) before any "successful" diffusive motion occurs.

As we increase further in frequency, we encounter the NCL regime. What does this sort of ac conductivity imply about the mean-squared displacement of ions? One might naively assume that the mean-squared displacement is given by Eq. (9) above with $n=1$ meaning that it is a time-independent constant. But this is incorrect. Instead, the NCL of the ac conductivity implies a logarithmic time dependence (Nowick *et al.*, 1998) for the mean-squared displacement of the form

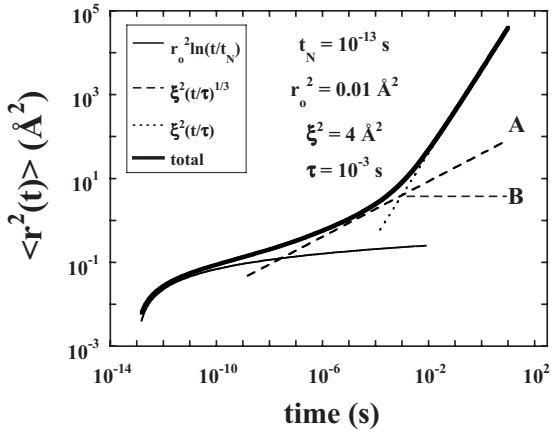

FIG. 3. Schematic representation of the time dependence for mean-squared displacement of ions corresponding to the ac conductivity in Eq. (6). Dashed line *A* corresponds to approximation used in Eq. (6). Dashed line *B* shows a more appropriate approach to a constant at long times as indicated by Eq. (14).

$$\langle r^2(t)\rangle_{\rm NCL} \propto \ln(t). \tag{10}$$

Since each of the three distinct regions of mean-squared displacement are well separated in time, we could model the entire time-dependent mean-squared displacement by a sum of the form

$$\langle r^2(t)\rangle_{\rm net} \approx r_0^2 \ln(t/t_N) + \xi^2(t/\tau)^{1-n} + \xi^2(t/\tau), \tag{11}$$

where r_0 and t_N are some appropriately short length and time scale, respectively, pertaining to the first regime of ion motion. This approximation also assumes that $t/t_N>1$, $t_N \ll \tau$, $r_0^2<\xi^2$, and $0<n<1$. An example of the resulting $\langle r^2(t)\rangle_{\rm net}$ is shown in Fig. 3. The benefit of modeling the net mean-squared displacement by the sum above is that one can *analytically* obtain [through Fourier transform in Eq. (3)] the corresponding real and imaginary parts of the ac conductivity,

$$\sigma'_{\rm ion}(\omega) = {\rm Re}\ \sigma^*(\omega) = \frac{Nq^2r_0^2}{6kT}\frac{\pi}{2}\omega + \frac{Nq^2\xi^2}{6kT}\frac{1}{\tau}\{1+\Gamma(2-n)\cos(n\pi/2) \times(\omega\tau)^n\}, \tag{12}$$

$$\varepsilon'_{\rm ion}(\omega) = \frac{1}{\omega\varepsilon_0}{\rm Im}\ \sigma^*(\omega) = \frac{Nq^2r_0^2}{6kT\varepsilon_0}[\ln(\omega_N/\omega)-\gamma] + \frac{Nq^2\xi^2}{6kT\varepsilon_0}\Gamma(2-n)\sin(n\pi/2)(\omega\tau)^{n-1}, \tag{13}$$

where $\omega_N=1/t_N$ and γ ($\approx 0.5772\ldots$) is Euler's constant. Although based on an approximate, asymptotic form for

the overall mean-squared displacement, these two expressions capture the essence of the experimentally observed ac conductivity. Unfortunately, Eq. (13) incorrectly predicts a continuous increase in $\varepsilon(\omega)$ with decreasing frequency instead of the approach to a plateau value $\varepsilon(0)$ (see Fig. 2). This is only a consequence of how the expression for $\langle r^2(t)\rangle_{\rm ac}$ in Eq. (9) fails at $t>\tau$, where, in analogy to a rotating dipole, the mean-square displacement associated with this ac contribution would approach a limiting constant. A more accurate representation for the ac contribution would then be

$$\langle r^2(t)\rangle_{\rm ac} \approx \begin{cases} \xi^2(t/\tau)^{1-n}, & t<\tau \\ \xi^2, & t>\tau, \end{cases} \tag{14}$$

which would remove the erroneous low-frequency divergence of ε'.

Experimentally, the length scale that corresponds to the crossover between diffusive and correlated motion is around $\xi\approx 2$ Å. But what is the typical value of r_0 in Eq. (12)? Combining Eq. (12) with Eq. (6), we find

$$A = \frac{Nq^2r_0^2}{6kT}\pi^2. \tag{15}$$

In a survey of the NCL, Ngai and Moynihan (1998) reported values of the parameter A in Eq. (6) for a diverse number of ion-conducting glasses. Of these, about 80% exhibited a value for A in a range from 0.8×10^{-12} to 20×10^{-12} S/m with an average of about 4×10^{-12} S/m. Using this average value together with the typical parameters employed previously ($N\approx10^{28}$ m^{-3}, $q=e$, $T=300$ K), we obtain a length scale $r_0\approx0.06$ Å. Such a small length scale is clearly inconsistent with mass transport processes but might be a reflection of the quasivibrational, anharmonic motion of the ion at very short times. Indeed, such an interpretation for the origin of the NCL has been advanced (Ngai, 1999).

IV. ALTERNATIVE INTERPRETATIONS AND REPRESENTATIONS

At this point we acknowledge that the study of ionic relaxation has a long history and that, while the ac conductivity affords direct contact with the mean-squared displacement of ions, several other alternative interpretations of the frequency dependence have been advanced (Moynihan, 1994; Ngai and Leon, 1999; Dyre and Schroder, 2000; Schroder and Dyre, 2000; Hodge *et al.*, 2005). Dyre (Dyre and Schroder, 2000; Schroder and Dyre, 2000) has obtained similar frequency-dependent conductivity and permittivity using effective medium approximation models that examine how the dielectric response of the entire system (ions and matrix) is affected by the applied field without reference to $\langle r^2(t)\rangle_{\rm ac}$. Along with these alternate interpretations have arisen other representations of the raw experimental data [i.e., $C(\omega)$ and $R(\omega)$]. Most popular among these is the electric modulus M^* formally defined as the inverse of the complex permittivity,

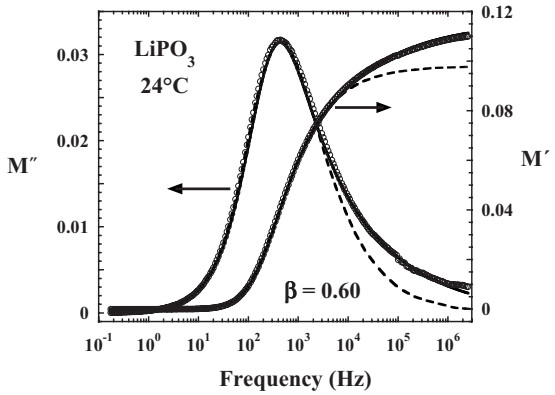

FIG. 4. Real and imaginary parts of the electric modulus for $LiPO_3$ glass near room temperature. The solid lines are a fit to Eqs. (12) and (13). The dashed line shows a fit to the KWW relaxation function with $\beta=0.6$.

$$M^*(\omega) \equiv \frac{1}{\varepsilon^*(\omega)} = M' + iM'' = \frac{\varepsilon'}{\varepsilon'^2+\varepsilon''^2} + i\frac{\varepsilon''}{\varepsilon'^2+\varepsilon''^2}. \tag{16}$$

The electric modulus was originally introduced by McCrum, Read, and Williams (1967) and was extensively developed by Macedo and co-workers (Macedo *et al.*, 1972; Provenzano *et al.*, 1972). The interested reader is directed to more recent articles regarding the electric modulus formalism (Macedo *et al.*, 1972; Ngai and Moynihan 1998; Ngai and Leon, 1999; Hodge *et al.*, 2005). Features of this data representation are displayed in Fig. 4, where both the real and imaginary parts of the modulus are plotted against frequency for a lithium metaphosphate glass near room temperature (Sidebottom *et al.*, 1995c). The features of the modulus shown in the figure are very typical: the real part of the modulus exhibits a steplike increase with increasing frequency and the imaginary part displays a peaked function that is usually broader than a Gaussian and considerably more asymmetric.

Early in its development, workers recognized that the simplest model for the conductor involving only a frequency-independent dc conductivity and a frequency-independent dielectric constant would generate moduli curves that were symmetric and only 1.14 decades wide [full width at half maximum (FWHM)]. This corresponds to a Debye relaxation $E(t)=E(0)\phi(t)=E(0)\exp(-t/\tau)$ of the electric field (inside the material) when a constant displacement field is maintained (Macedo *et al.*, 1972). Experimentally, the electric modulus is rarely ever this narrow nor this symmetric, and it was suggested (Macedo *et al.*, 1972) that the exponential decay be replaced by a nonexponential decay function $\phi(t)=\exp[-(t/\tau)^\beta]$. In analogy to mechanical relaxation, the frequency-dependent electric modulus is

$$M^*(\omega) = \frac{1}{\varepsilon_\infty}\left\{1 - \int_0^\infty dt\,\exp(-i\omega t)\left(-\frac{d\phi}{dt}\right)\right\}. \tag{17}$$

Although analytic solutions of the Laplace transform are not possible for the decay function above, numerical

tables of the normalized curves for a variety of stretching exponents are available (Moynihan *et al.*, 1973). An example of using this stretched exponential decay function to fit the modulus data is shown in Fig. 4. Also shown for comparison is a fit using Eqs. (12) and (13) (but omitting the NCL terms in these expressions). A recurrent failure of the stretched exponential is that it almost always underestimates the high-frequency data [usually starting some 1.5 decades beyond the peak frequency (Moynihan, 1994; Nowick and Lim, 1994)].

V. SCALING PROPERTIES OF THE IMPEDANCE MEASUREMENTS

Now the stage is set. We have spectra of raw data represented either as ac conductivity or as moduli and seek to understand what they convey about ion motion. We could at this stage collect our measurements and proceed with curve-fitting approaches such as the stretched exponential for the modulus or fits of Eqs. (12) and (13) or others (Macdonald, 2007) to the conductivity to obtain relevant parameters that characterize the ion motion. However, our purpose is to explore the minimalist approach of comparing spectra against one another to see what can be learned first.

Returning to the frequency dependence of the ac conductivity and dielectric constant shown in Fig. 2 (or its Fourier transform counterpart shown in Fig. 3), we ask how is the corresponding pattern of $\langle r^2(t)\rangle$ affected by a change in the temperature? Stated another way, if the approximate form represented by Eq. (11) provided a valid representation for $\langle r^2(t)\rangle$, does changing temperature affect the length scales, time scales, or both? Many dynamical processes in disordered materials exhibit what is often referred to as "thermorheological simplicity" (TRS), also known as "time-temperature superpositioning." This means that although the characteristic frequency (or time) scale governing the process may vary with temperature, the inherent spectral features of the relaxation remain in their same proportion. Consequently, the frequency-dependent shape of the relaxation is undistorted by changing temperature and is only shifted in frequency (or time) by virtue of the temperature dependence of the characteristic frequency (or time).

The scaling of the ac conductivity requires both division by the dc conductivity (σ_0) and shifting by some characteristic frequency f_0',

$$\frac{\sigma}{\sigma_0} = F(f/f_0'). \tag{18}$$

Here the characteristic frequency f_0' refers to any arbitrary frequency that coincides with a specific marker on the $\sigma(\omega)$ curve. A common choice (Kahnt, 1991) is the frequency f_0 defined in Eq. (6) for which

$$\sigma(f_0) = 2\sigma_0. \tag{19}$$

An example of scaling the data for a sodium germanate glass at a series of different temperatures is shown in Fig. 5. In this scaled representation, the data collapse to a common curve, a so-called master curve, whose shape is given by the function $F(x)$ in Eq. (18).

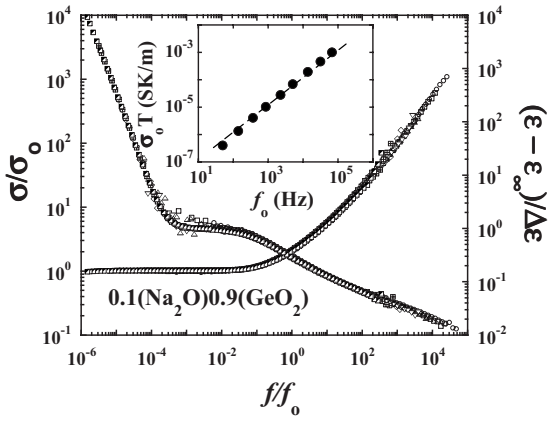

FIG. 5. Scaling plot of both the ac conductivity and ac permittivity of $(Na_2O)_{10}(GeO_2)_{90}$ demonstrating the collapse of individual spectra collected at different temperatures onto a master curve. Inset: The proportionality that is maintained between the vertical and horizontal scales of the ac conductivity in this instance of canonical scaling.

The scaling of the ac conductivity requires both a horizontal shift (f_0') and a vertical shift (σ_0). As it happens, these two scales are generally related by the Nernst-Einstein relation as

$$\sigma_0 T = (Nq^2\xi^2/6k)f_H = K(N,q,\xi)f_H. \tag{20}$$

Provided the quantity in parentheses $K(N,q,\xi)$ remains constant, then the product $\sigma_0 T$ will be proportional to the hopping frequency and, in kind, proportional to the horizontal scale f_0'. We refer to this sort of situation as the canonical case. Specifically, we refer to *canonical scaling* as that in which (i) the shape of the master curve is preserved [also implying that any measure of the shape like the exponent n in Eq. (6) remains fixed] and (ii) the vertical and horizontal scales are related by

$$\sigma_0 T \propto f_0'. \tag{21}$$

This sort of scaling is also referred to as "Sommerfield scaling" by Roling (Murugavel and Roling, 2002) and is merely a consequence of the constancy of the variable $K(N,q,\xi)$ in the Nernst-Einstein result above. This type of scaling is most often observed in temperature-dependent measurements of a sample of fixed ion concentration provided the disordered matrix remains *isostructural*. That is, the change in temperature, at most, results in a slight expansion of the material [causing counterpropagating changes to N and ξ in the variable $K(N,q,\xi)$] without causing any drastic alteration of the local environment of the ion. The proportionality between $\sigma_0 T$ and f_0' for our data in Fig. 5 is demonstrated in the inset.

At this time we also establish a nomenclature for two other related scenarios we will discuss. The first we refer to as *semicanonical* scaling. We define this sort of scaling to pertain to those situations in which (i) the shape of

the master curve is preserved, but (ii) the vertical and horizontal scales are not proportional. This scaling situation arises in instances where either the ion concentration or hopping distance [the quantities N and ξ in the variable $K(N,q,\xi)$] is changing. The last situation we refer to as *anomalous*. This pertains to those rarer situations in which the shape of the ac conductivity curve is changing and so a collapse to a common master curve cannot obtained. These situations are typically associated with changes occurring in the glass structure in the vicinity of the ion.

Before we discuss specific examples of semicanonical scaling and the anomalous cases, we first tidy up a remaining thread associated with the scaling of the ac conductivity. Since the ac conductivity is a complex quantity, its imaginary part (the real part of the dielectric permittivity) should also exhibit TRS. This part of the impedance response also includes the nonionic contribution ε_∞ due to faster polarization processes, so we would only anticipate TRS to be seen for the ionic-only quantity $\varepsilon'(\omega)-\varepsilon_\infty$. A scaling ansatz of the form

$$\frac{\varepsilon' - \varepsilon_\infty}{\Delta\varepsilon} = G(f/f_0') \tag{22}$$

was seen to work well (Sidebottom and Zhang, 2000), and an example of this scaling is included in Fig. 5 for the sodium germanate glass. As it turns out, this second scaling function $G(x)$ is related to $F(x)$ via the Kramers-Kronig relations (Jackson, 1975). Without going into the details, one can show that these relations require

$$f_0' = \frac{\sigma_0}{2\pi\varepsilon_0\Delta\varepsilon}. \tag{23}$$

Again, f_0' and f_0 are fundamentally the same representation of a characteristic frequency scale, each proportional to the ionic hopping rate f_H.

An interesting feature of the scaling that emerges from the Kramers-Kronig analysis is how the two vertical scales [σ_0 in Eq. (18) and $\Delta\varepsilon$ in Eq. (22)] are constrained by the common horizontal scale (f_0). This relationship is not entirely new but was seen experimentally in earlier work. There it is referred to as the Barton-Nakajima-Namikawa relationship (Tomozawa, 1977). The relationship is also predicted by certain theoretical models (Dyre, 1986, 1993).

This Barton-Nakajima-Namikawa relation can also be combined with the Nernst-Einstein relation [Eq. (20)] to obtain an expression for the step increase occurring in the dielectric constant $\Delta\varepsilon$. To within some factor of order unity,

$$f_H \approx \frac{\sigma_0}{\varepsilon_0\Delta\varepsilon}. \tag{24}$$

Upon substituting this into Eq. (20), one obtains

$$\Delta\varepsilon T \approx Nq^2\xi^2/6\varepsilon_0 k = K(N,q,\xi)/\varepsilon_0, \tag{25}$$

a result that is essentially equivalent to our earlier approximation [see Eq. (5)] based upon the analogy of ion hopping to the rotational motion of dipoles with moment $p=q\xi$.

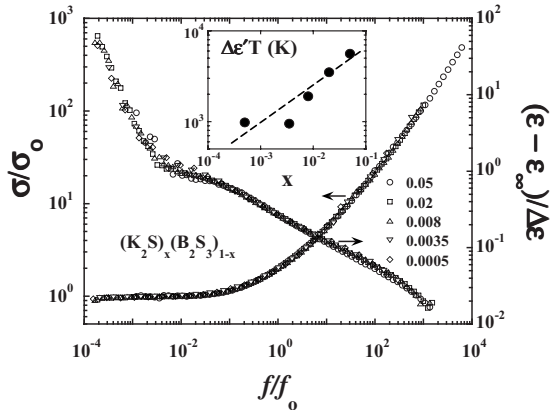

FIG. 6. Scaling plot of both the ac conductivity and ac permittivity of a series of potassium thioborate glasses demonstrating the collapse of the master curves of individual spectra collected at different temperatures for given ion concentration onto a master master curve for all ion concentrations. Inset: The variation of $\Delta\varepsilon T$ with ion concentration. The dashed line corresponds to a variation of $\Delta\varepsilon T \approx x^{0.4}$.

VI. EXAMPLES OF SEMICANONICAL SCALING

A. Alkali thioborates

In 1992, Patel and Martin (1992a, 1992b) studied the ionic relaxation of sodium thioborate glasses, $(Na_2S)_x(B_2S_3)_{1-x}$, in which the concentration of ions varied from $x=0.001$ to 0.15. Additional measurements on a similar series of potassium thioborate glasses can be found in Patel (1993). What is particularly unique about the study is the extreme variation in ion concentration that spans over two orders of magnitude. An obvious question is: How does such a large change in the ion concentration affect the correlated motion?

In Fig. 6 we show the scaling of the both the conductivity [Eq. (18)] and dielectric constant [Eq. (22)] that can be obtained for the series of potassium thioborate glasses ranging from $x=0.0005$ to 0.05 mole fraction. Hidden in this figure is a twofold level of scaling. First, for each composition there is a canonical scaling of the spectra obtained at different temperatures onto a master curve. Second, these master curves for each composition are then superimposed to produce yet another master curve—a "master" master curve. An especially significant outcome of the scaling is that it clearly demonstrates how the shape of the curve (i.e., the nature of the correlated ion motion) is not influenced by even a two orders of magnitude change in the ion density. This finding proves conclusively that the correlated motion is not a consequence of any interaction between mobile ions.

Figure 7 shows plots of $\sigma_0 T$ vs f_0 for the glasses scaled in Fig. 6. The slope of each curve is linear (indicating the canonical scaling for each composition alone) but the curves are individually shifted such that the proportionality constant between these two quantities $K(N,q,\xi)$ is

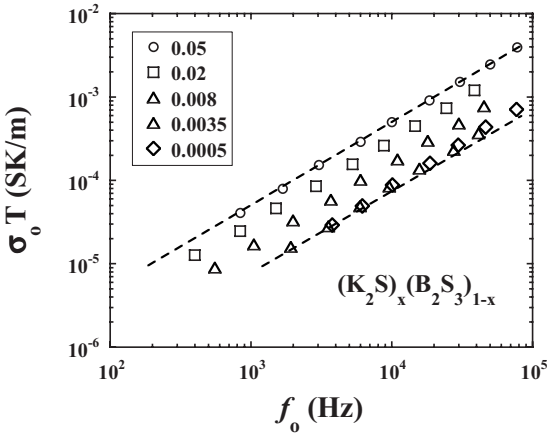

FIG. 7. The dc conductivity (multiplied by the temperature) vs the scaling frequency for a series of potassium thioborate glasses showing how canonical scaling is present in each composition, but that the proportionality constant $K(N,q,\xi)$ is systematically changing from one concentration to the next.

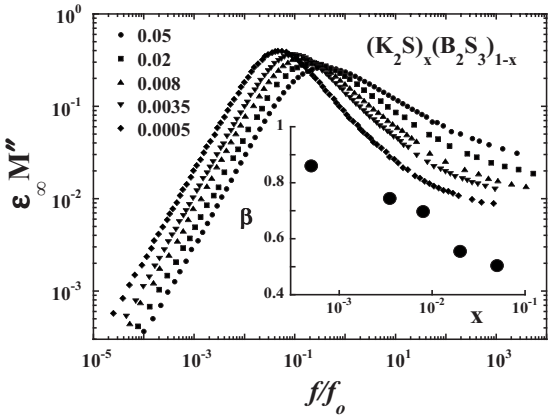

FIG. 8. Real part of the electric modulus for the series of potassium thioborate glasses shown in previous figures. Here the modulus is multiplied by the high-frequency dielectric constant and the frequencies have been scaled as before in Fig. 6. Inset: The compositional variation of the stretching exponent.

clearly dependent on the ion concentration. As the inset to Fig. 6 reveals, this proportionality constant [here represented by the quantity $\Delta\varepsilon T$; see Eq. (25)] increases with increasing ion concentration as x^a, where $a \approx 0.4 \pm 0.1$. At first sight, this nonlinear variation of $K(N,q,\xi)$ is not expected since in Eq. (25) $K(N,q,\xi)$ is only proportional to N. However, a simple interpretation for this particular concentration dependence is that the thioborate glasses behave in an isostructural manner such that the ion hopping length is uniformly increased by decreasing N. In other words, the lattice of charge-compensating sites experiences a spatial expansion causing an increase in the distance ($\xi \approx N^{1/3}$) an ion must hop to reach an adjacent charge-compensating site in the network. When this N dependence for ξ is included, one anticipates $K(N,q,\xi) \approx x^a$, with $a \approx 0.33$. This predicted value is quite close to that seen above for the potassium thioborates (Sidebottom, 1999a) and was also reported by Roling (1998) for a series of sodium germanate glasses at low ion concentrations.

The scaling behavior of the ac conductivity and the permittivity shown in Fig. 6 must be contrasted with the behavior of the electric modulus as shown in Fig. 8. In this plot, the imaginary part of the electric modulus for the thioborate glasses has been normalized by the high-frequency permittivity (ε_∞) and the frequency scaled by the same characteristic frequency f_0 used in Fig. 6. Clearly evident in the figure is a systematic evolution in the shape of the high-frequency wing of the modulus which is caused by changes in the ion concentration. In short, the modulus fails to display thermorheological simplicity. In the inset are the values of the stretching exponent (β) obtained by fitting [Eq. (17)] with the stretched exponential relaxation. Many advocates of the electric modulus formalism consider the shape changes in the electric modulus to be evidence that the correlated ion motion is a result of coupling between mobile ions. Naturally, such a coupling between ions would decrease with decreasing ion concentration, and it has been proposed in certain empirical models (Ngai, 1979; Ngai and Rendell, 1991; Ngai and Kanert, 1992) that the absence of such coupling would result in exponential relaxation. Nevertheless, this interpretation is in direct conflict with that obtained above from consideration of the ac conductivity.

B. CKN

We consider another semicanonical situation. This one involves the ionic melt composed of two nitrate salts: $0.4Ca(NO_3)_2$-$0.6KNO_3$ (CKN). This glass-forming material has been a favorite of glass researchers (Howell *et al.*, 1974; Pimenov *et al.*, 1996; Sidebottom and Zhang, 2000) and because of its nonrefractory glass transition temperature, impedance measurements can be readily obtained for CKN both in the glass and in the supercooled liquid state. Once again an obvious question would be: To what extent does the transition from liquid to solid affect the correlated motion of ions?

Figure 9 shows the ac conductivity and permittivity of CKN scaled to master curves in the same fashion as for the previous examples. What is particularly significant is that the individual spectra span a range of temperatures from below the glass transition (open symbols) to well above the glass transition (filled symbols). With the exception of the region dominated by the electrode polarization, the curves superimpose to form a master curve both above and below T_g. Hence the transition from glass to liquid does not affect the nature of the correlated ion motion.

Figure 10 shows the variation of $\sigma_0 T$ with respect to the scaling frequency f_0 for CKN. Far from T_g, these two quantities appear to be proportional as indicated by the dashed lines of unit slope shown in Fig. 10. However, despite the fixed composition of the material, this simple proportionality is not retained through the transition region. It stands to reason that the failure of canonical

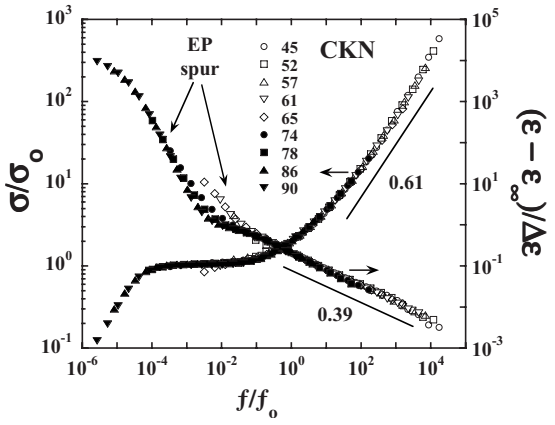

FIG. 9. Scaling plot of both the ac conductivity and ac permittivity of CKN demonstrating the collapse of individual spectra collected at different temperatures, both above and below the glass transition, onto a master curve. The two lines indicate the approximate power-law exponents seen near f_0.

scaling in this instance must again be a reflection of changes in the quantity $K(N,q,\xi)$. As shown in the inset to Fig. 10, $K(N,q,\xi)$ (here represented again by $\Delta\varepsilon T$) experiences a roughly fourfold increase across the glass transition. One explanation offered for this is that changes are occurring near the glass transition in the populations of ions that are sufficiently mobile to produce a significant contribution to the conductivity (Sidebottom and Zhang, 2000). It should be realized that the observed ac conductivity is a composite of all mobile ion species present in the sample. It just so happens that our last two examples (sodium germanate and potassium thioborate) involve network glasses for which the charge-compensating sites are affixed to the network and only a single alkali cation species is mobile. Since the charge-compensating sites do not hop about, they make no contribution to the ac conductivity [except pos-

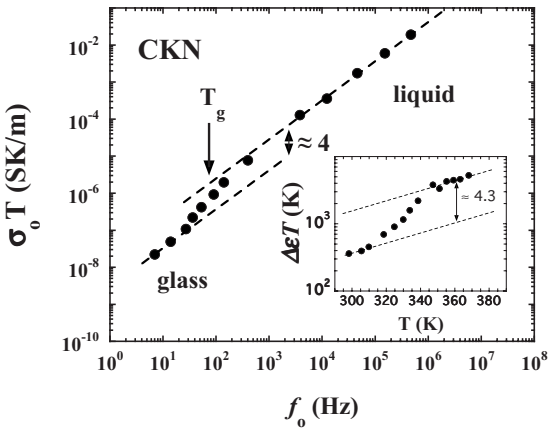

FIG. 10. The dc conductivity (multiplied by the temperature) (vs) the scaling frequency for CKN showing how a canonical scaling is present both above and below the glass transition, but that the proportionality constant $K(N,q,\xi)$ is systematically changing in the transition range by roughly a factor of 4.3. Inset: The corresponding variation of $\Delta\varepsilon T$ with temperature near $T_g \approx 60\,^{\circ}$C.

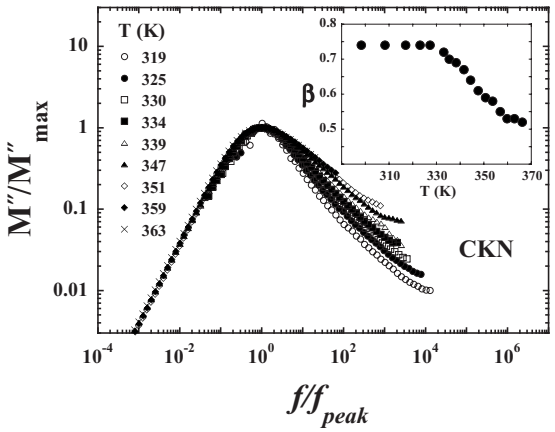

FIG. 11. The real part of the electric modulus for the CKN data shown in Fig. 10. Here the modulus is scaled to its maximum value and the frequencies have been scaled to the frequency of the maximum in M''. Inset: The temperature variation of the stretching exponent reported by Howell (Howell *et al.*, 1974).

sibly in the NCL region where very small displacements become significant (Sidebottom, 2005)]. However, in CKN all charge entities are, in principle, mobile and could contribute to the total response. Clearly, for CKN to be solid below T_g, some atoms will have to be strictly immobile. However, above T_g, we have a liquid for which all atoms are mobile over some time frame. Thus we can associate the shift in Fig. 10 with this necessary increase in the number of mobile ions.

Again, we contrast this scaling of the conductivity with the behavior of the electric modulus. For CKN the shape of the electric modulus changes near the glass transition, as shown in Fig. 11. Below T_g, the shape is approximately fixed and its best description using the stretched exponential yields $\beta=0.72$. However, in the liquid above T_g, this β value decreases with increasing temperature. The variation of β with temperature is shown in the inset to Fig. 11 for measurements by Moynihan (Howell *et al.*, 1974). Thus once more we find a stark disagreement between the conductivity and modulus formalisms over the important issue of thermorheological simplicity.

VII. SCALING OF THE ELECTRIC MODULUS

It is evident from our two semicanonical examples above that the electric modulus and conductivity formalisms do not agree as to the presence or absence of TRS. On the surface of it, the result is quite puzzling as both data representations are spawned from the same raw data [$R(\omega)$ and $C(\omega)$]. To see how this arises, we must examine the electric modulus more closely. Because the modulus is defined in such a way as to include the *nonionic*, high-frequency permittivity ε_∞, in addition to the ionic contributions, it cannot *a priori* be expected to obey TRS, especially in these semicanonical situations.

To demonstrate the truth of this statement, it is a simple matter to consider how the TRS behavior of Eqs.

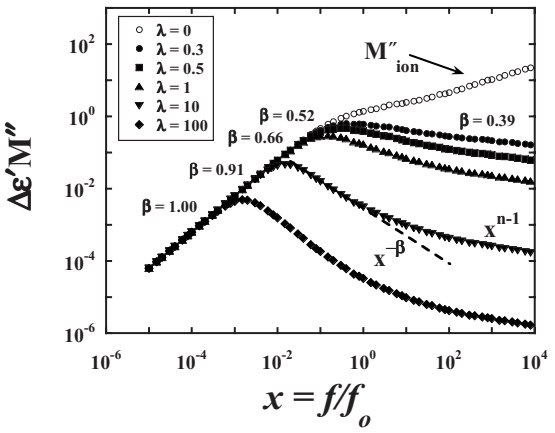

FIG. 12. Construction of the imaginary part of the electric modulus from the scaling forms for the conductivity [Eq. (18)] and permittivity [Eq. (22)]. This demonstrates how the shape of the modulus is sensitive to the quantity $\lambda=\varepsilon_\infty/\Delta\varepsilon$. Corresponding values of the stretching exponent are also provided for comparison.

(18) and (22) is afflicted when the modulus is defined either with or without ε_∞. Without ε_∞, the modulus would be the "ionic only" modulus

$$M^*_{\text{ion}}(\omega) \equiv \frac{1}{\varepsilon^*(\omega) - \varepsilon_\infty}. \tag{26}$$

Using the scaling forms [see Eqs. (18) and (22)] seen to hold experimentally for $\sigma(f)$ and $\varepsilon(f)$, the imaginary part of this ionic modulus would be

$$M''_{\text{ion}}(\omega) = \frac{1}{\Delta\varepsilon}\frac{F(x)/2\pi x}{[G(x)]^2 + [F(x)/2\pi x]^2} = \frac{1}{\Delta\varepsilon}H(x), \tag{27}$$

where $x=f/f'_0$. Clearly, this ionic modulus can be described by a master curve and it does in fact scale for the two examples discussed earlier (Sidebottom *et al.*, 2000).

But now consider the electric modulus with ε_∞ included, as it is conventionally defined. The imaginary part of this modulus becomes

$$M''(\omega) = \frac{1}{\Delta\varepsilon}\frac{F(x)/2\pi x}{[\lambda + G(x)]^2 + [F(x)/2\pi x]^2} = \frac{1}{\Delta\varepsilon}H_\lambda(x), \tag{28}$$

where $\lambda=\varepsilon_\infty/\Delta\varepsilon$. It is clear that when the modulus is defined to include the ε_∞, it develops a subsequent dependence upon $\Delta\varepsilon$ [and hence $K(N,q,\xi)$] as well. The modulus, as it is defined here, will display TRS only if the quantity λ remains constant. To explore this further, examples of the shape of the modulus obtained from Eq. (28) are presented in Fig. 12 for a selection of values for the parameter λ, including the case of $\lambda=0$ for which Eq. (28) is seen to reduce to that of M^*_{ion} in Eq. (27). The figure reveals a radical change wrought on the ionic modulus by the inclusion of ε_∞, in which a monotonic function of frequency folds over to become a peaked function (Elliott, 1994b). Also shown in the figure are the stretched exponents β for fits of Eq. (17). One sees that as λ increases, the β exponent approaches unity and for values of λ of order unity, $\beta\approx0.6$, a value that has been commonly observed (Ngai and Martin, 1989; Ngai *et al.*, 1989, 1998). Thus the absence of TRS in the modulus (occurring in situations of semicanonical scaling for conductivity) is traced to its original definition that includes nonionic polarization.

VIII. ABSENCE OF SCALING

For both the canonical and semicanonical situations, the reader is reminded that master curves can be obtained and it is only an issue of whether the quantity $K(N,q,\xi)$ defined earlier remains constant (canonical) or changes (semicanonical). We now want to look into exceptions to the scaling—what we refer to as anomalous scaling—in which a master curve cannot be obtained by any combination of vertical and horizontal scaling. These cases are of fundamental significance as they represent situations in which the intrinsic process of ion motion is being altered in some manner. A study of the systematic changes in the shape of the conductivity curve will, in principle, offer insight into the nature of the correlated ion motion in these disordered conductors.

Before beginning this discussion, it should be acknowledged that any simple parametrization of the shape of the conductivity curve will be wanting. The curve often covers extensive ranges of frequency and conductivity, and even an empirical fit function such as Eq. (6) (while able to account for the basic shape over some 20 square decades to within 5%) commonly fails to describe the details in the vicinity of f_0 where the crossover from correlated to diffusive motion occurs (Sidebottom, 1999b). Although other schemes for parametrizing the shape have been devised (Roling and Martiny, 2000; Schroder and Dyre, 2000), the most common parametrization of the shape of the curve is the exponent n obtained through curve fitting by Eq. (6). The main advantage of this description for the shape is that it provides a single number that can be tabulated and readily compared among a wide diversity of materials. An obvious drawback of this parametrization is that it lacks precision owing to the fact that the slope of $\sigma(\omega)$ is *continually* increasing at high frequencies as the NCL regime is approached. Nevertheless, if the fitting of $\sigma(\omega)$ is restricted to a regime near the crossover from correlated to diffusive, say for frequencies below about $10^3 f_0$, a good measure of the shape can be reliably obtained.

A. Borate and germanate anomalies

A first example of anomalous scaling arises in the conductivity studies by Roling (Roling and Martiny, 2000) of alkali borate and alkali germanate glasses of varying ion content. In the study of borate glasses, the sodium content varied from 10 to 30 mol % alkali oxide. For every one of these compositions, the $\sigma(\omega)$ curve at various temperatures could be scaled (canonically) to an indi-

vidual master curve. However these master curves, obtained from different compositions, could not be completely collapsed together onto a master master curve. Although a collapse could be obtained at both high and low frequencies, systematic changes in the shape occurred in the crossover region near f_0. In the companion study of sodium germanate glasses (Roling *et al.*, 1999) for which the alkali oxide content varied from approximately 1 to 40 mol %, attempts to obtain a master master curve were similarly unsuccessful.

A puzzle arises as to why the shape of $\sigma(\omega)$ changes as the ion concentration of these glasses is altered when no such shape changes were evident either in the thioborate study or in a study of sodium germanates at ultralow ion concentrations (Sidebottom, 1999b). The resolution seems to be that the shape of $\sigma(\omega)$ is preserved in all these systems provided the ion concentration remains below those levels where well-documented changes in the network structure of the glass occur. In both the alkali borate and germanate systems, the addition of alkali oxide initially results in increased polymerization of the oxide network. For B_2O_3, the initial addition of alkali oxide results in conversion of BO_3 units to BO_4 (Krogh-Moe, 1965; Shelby, 1983). That is, the added oxygen atom *forms* a bridging bond that further polymerizes the network and hence increases the glass transition temperature. In a similar way, addition of alkali oxide to GeO_2 results in conversion of four-coordinated Ge to six-coordinated Ge with a concomitant increase occurring in the glass transition temperature (Huang and Jain, 1995; Jain *et al.*, 1996). For both the borate and germanate systems, higher levels of alkali addition eventually lead to the formation of nonbridging oxygens (NBOs) that depolymerize the structure and lower T_g.

It would appear then that the correlated motion is sensitive to properties of the charge-compensating site to which the mobile ion is tethered. At very low ion concentrations, these sites all appear identical in the borate and germanate glasses (either BO_4 or GeO_6 and little or no NBOs). Consequently, the initial increase in the ion concentration produces only simple, isostructural, changes in N and ξ that only affect the vertical and horizontal scaling of the conductivity curve without altering the shape. As the ion content increases to levels near the borate and germanate anomalies, the environment of the tethered ion is no longer identical from one site to the next, but can be either one of high oxygen coordination or one involving a NBO. It seems that these changes in the local environment of the mobile ion produce measurable changes in the correlated motion and in turn obfuscate the collapse of $\sigma(\omega)$ to a common master curve.

B. Mixed alkali effect

Another well-documented case of anomalous scaling involves the so-called mixed alkali effect (MAE). For many years researchers have highlighted the dramatic decrease in the dc conductivity (often by several orders of magnitude) that results in alkali oxide glasses when half of the alkali ions are simply replaced by ions of another species (say Li replaced by Na) (Day, 1976; Ingram, 1994). A number of studies of the ac conductivity clearly show an alteration occurring in the shape of $\sigma(\omega)$ when the mixing ensues (Sidebottom, 1999c; Roling and Martiny, 2000). For the unmixed (single alkali) situation, the exponent n is around 0.67 but decreases to about 0.60 when ions are mixed (Sidebottom, 1999c).

Could the origin of this shape change also stem from some nonuniformity of the local environment of the charge-compensating site like that which occurs near the borate and germanate anomalies? The best current interpretation of the MAE is based upon the notion that the local environment of the charge-compensating site is specifically configured to accommodate a particular mobile ion (ion A or ion B) and that there is an energy penalty associated with any transition of an A ion into a B-configured site or vice versa (Greaves, 1989; Bunde *et al.*, 1991; Maass *et al.*, 1992). This energy penalty arises from the need for the lattice to mechanically relax whenever the ion enters or leaves an ill-configured site, and it is the source for the dramatic decrease in the total ion diffusivity. Here again it seems that changes occurring in the mobile ion's local environment impact the nature of its correlated motion.

C. Constriction effect

One final example of anomalous scaling regards the ac conductivity of certain alkali metaphosphate and halide-doped metaphosphate glasses (Sidebottom, 2000). In the series of $(AgI)_x(AgPO_3)$ glasses, the shape of $\sigma(\omega)$ changed systematically from a shape characterized by $n \approx 0.59$ at $x=0$ to $n \approx 0.67$ at $x \geqslant 0.3$. This increase in n appears to correlate to the spreading apart of the phosphate chains that occurs when the iodine atom is incorporated (interstitially) into the structure. In the series of MPO_3 (M=Li,Na,K,Rb,Cs) glasses, the exponent was observed to decrease from $n \approx 0.67$, seen for both the $LiPO_3$ and $NaPO_3$ glasses, to about 0.54 for glasses containing larger cations.

For both these metaphosphate systems it was shown that the changes in n could be directly correlated to changes occurring in the level of "constriction" of the mobile ion, defined as a ratio of the size of the mobile cation to the mean spacing between the phosphate chains. This correlation is shown in Fig. 13. Unlike the anomalous scaling for the borate and germanate anomalies discussed above, here there are really no comparable changes occurring in the structure of the charge-compensating site. For the alkali metaphosphate glasses, these charge-compensating sites consist of the two terminal oxygens that reside on each P atom. Instead, the changes in the ion's local environment involve changes in the relative number of degrees of freedom available for local ion motion.

To what extent can we generalize these situations of anomalous scaling? A common thread that links all

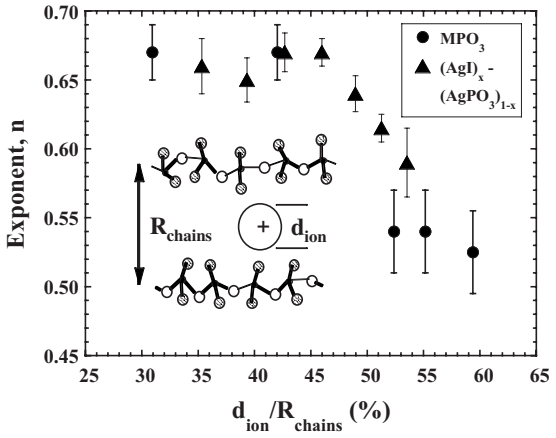

FIG. 13. The conductivity exponent observed in metaphosphate glasses as a function of the constriction (i.e., ratio of the cations' size to the mean spacing between phosphate chains).

these examples suggests the anomaly stems from changes in the local environment as seen by the mobile ion. In the constriction situation, it seems that the change in the correlated motion is linked to a change in the effective dimensionality of the conduction space; the exponent n decreases as that dimensionality decreases (Sidebottom, 2000).

To obtain a wider perspective on this connection, it is insightful to examine the shape of the ac conductivity seen in those ion-conducting materials for which the conduction space is decidedly other than three dimensional. Examples include sodium β-alumina (Almond *et al.*, 1982) in which conduction of the Na cation occurs in the two-dimensional space in between the alumina planes, and hollandite (Bernasconi *et al.*, 1979; Iwauchi and Ikeda, 1992), in which conduction is restricted to one dimension along channels. In Fig. 14 a plot of the power-law exponent n for these and other ion-conducting materials is shown as a function of the effective dimensionality of the conduction space. In the plot, mixed alkali and halide-doped glasses have been assigned an intermediate dimensionality (Sidebottom, 1999d). Evident from the figure is a trend that supports

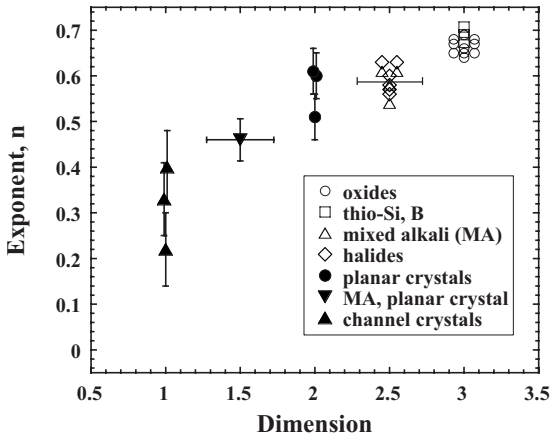

FIG. 14. The conductivity exponent vs the effective dimensionality of the local conduction space.

the contention that correlated ion motion is largely controlled by the effective dimensionality of the local conduction space. It should be emphasized that since the correlated motion occurs only on length scales of about 2 Å (somewhat larger for glasses of ultralow ion content), it is only the effective dimensionality of this local conduction space in the vicinity of the charge-compensating site that matters.

IX. NEARLY CONSTANT LOSS

Presently there is intense effort made to better understand the origins of the last term in Eq. (15), known as the nearly constant loss (NCL). As originally noted by Jonscher (1977), the NCL behavior is endemic to most solids: amorphous and crystalline, ionic and dipolar. In 1994, many researchers (Svare *et al.*, 1993; Kanert, Kuchler, Dieckhofer, *et al.* 1994; Kanert, Kuchler, Nagi, and Jain, 1994) focused attention on this dynamic regime using both impedance and nuclear spin relaxation techniques. At that time it was suggested that the NCL arose from some form of low-energy excitation that could be described by a transition within an asymmetric, double-well potential (Lu and Jain, 1994). More recently, Ngai (1999) conjectured that the NCL may be related to the short-time dynamics in glassy materials that makes up the Debye-Waller factor, in turn related to the anharmonicity of the interaction potential.

In any event, while there are examples of the NCL in materials that are nonionic, there is also clear evidence that ionic materials exhibit a NCL behavior as a direct result of the ion motions. Since the purpose of this discussion is to examine how impedance spectroscopy can be used as an experimental technique for studying ion motion, our focus here is toward the issue of how the NCL due to ion motions can be distinguished from the NCL due to other, nonionic, polarizations. As we will see, the scaling properties of the ionic motions discussed previously feature prominently in our strategy for separating ionic from nonionic contributions to the dielectric loss. In this final section, we review two examples in which a nonionic contribution could be identified by considering the scaling properties of the data.

A. Sodium germanates

In a study conducted on a series of sodium germanate glasses $(Na_2O)_x(GeO_2)_{1-x}$, in which x ranged from 0.003 to 0.1, the ac conductivity was measured and shown to exhibit semicanonical scaling (Sidebottom and Murray-Krezan, 2002). At temperatures where the first term in Eq. (6) dominates, the conductivity could be collapsed to a common master curve, a curve whose slope approached unity at high frequencies. However, as one cools further into the NCL regime, the construction of the master curve becomes increasingly ubiquitous. Unlike the individual spectra obtained at higher temperatures, which display two distinct frequency dependencies above and below f_0, the spectra obtained at lower temperatures appear as a stretch of linear-frequency-

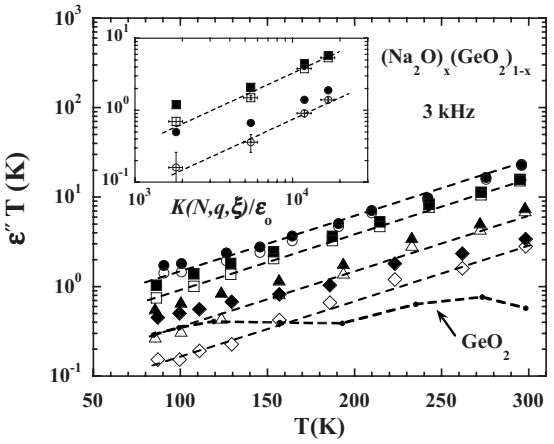

FIG. 15. The dielectric loss (multiplied by the temperature) for series of $(Na_2O)_x(GeO_2)_{1-x}$ glasses including the undoped GeO_2. Solid symbols are raw data. Open symbols are with the loss from GeO_2 subtracted. Inset: The vertical displacement of the loss at 100 and 200 K proportional to the value of $K(N,q,\xi)$ when the nonionic loss due to GeO_2 is first removed.

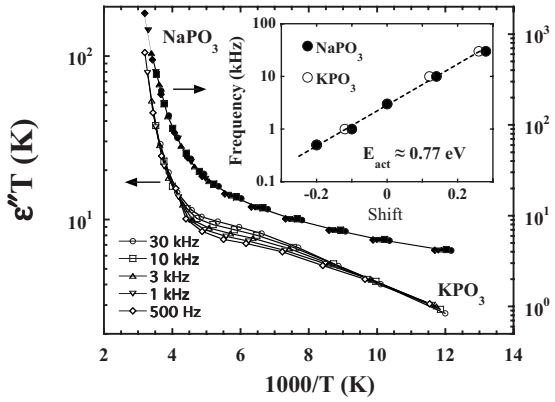

FIG. 16. The dielectric loss at five selected frequencies (multiplied by the temperature) for both $NaPO_3$ and KPO_3 glass. The individual isochronal spectra have been shifted along the ordinate axis so as to produce the best collapse to the curves at 3 kHz. Inset: The required shift factors and corresponding dc activation energy.

dependent conductivity. Thus the requisite vertical and horizontal shifts needed to position the spectrum onto the master curve, which were obvious for the high-temperature spectra, become arbitrary for the low-temperature spectra as the crossover regime is no longer visible within the window of the experiment. To circumvent this problem, we turn to the dielectric loss $\varepsilon''(\omega)$. If we rewrite the scaling of the ac conductivity given in Eq. (18) in terms of the dielectric loss using Eq. (2), we obtain

$$\varepsilon'' = \frac{\sigma}{\omega\varepsilon_0} = \frac{\sigma_0}{f_0' 2\pi (f/f_0')\varepsilon_0} F(f/f_0') = \frac{\sigma_0}{\omega_0\varepsilon_0}\left[\frac{F(f/f_0')}{(f/f_0')}\right]$$
$$= \frac{\sigma_0}{\omega_0\varepsilon_0}\tilde{F}(f/f_0'). \tag{29}$$

This can be tidied up using Eqs. (23) and (25) to replace the prefactor,

$$\varepsilon'' = \Delta\varepsilon\tilde{F}(f/f_0') \quad \text{or} \quad \varepsilon''T = \Delta\varepsilon T\tilde{F}(f/f_0')$$
$$= \frac{K(N,q,\xi)}{\varepsilon_0}\tilde{F}(f/f_0'). \tag{30}$$

This last form reveals an important feature to scaling the dielectric loss: in situations of canonical scaling, in which the quantity $K(N,q,\xi)$ is constant, individual spectra of $\varepsilon''T$ can be scaled onto a master curve with only a *horizontal* shift. This removes the ambiguity of the horizontal-plus-vertical shift required for scaling of $\sigma(f)$.

This sort of scaling was applied to the sodium germanate glasses. In Fig. 15 we show the temperature dependence of $\varepsilon''T$ for four glass compositions of varying ion concentration together with the undoped GeO_2 glass. Evident in the GeO_2 spectrum are low loss peaks. These losses from the base glass matrix contribute to the loss arising from ion motions. On the logarithmic scale shown, the data tend to compress together at lowest temperatures for samples containing the lowest ion concentrations. If, however, the loss from the GeO_2 sample is subtracted from the measured loss, as shown in Fig. 15, the remainder (the ionic portion) is seen to remain evenly spaced by an amount proportional to the quantity $K(N,q,\xi)$. This is demonstrated in the inset to Fig. 15. Thus, we are able to use scaling properties of the ionic motion to discern ionic from nonionic contributions in the NCL regime.

B. Alkali metaphosphates

Another example in which scaling properties are exploited to help identify nonionic contributions to the NCL is found in a recent study of the alkali metaphosphate glasses discussed earlier. When measurements of the dielectric loss of these glasses were extended to cryogenic temperatures, the temperature dependence displayed two variations depending upon the alkali ion (Sidebottom, 2005). For the small alkali, the dielectric loss decreased monotonically while the larger cations (K, Rb, Cs) exhibited a weak maximum between 200 and 80 K.

For this study, an ac capacitance bridge was employed to obtain the higher precision needed for the low loss exhibited in this temperature range. As a consequence, only about two decades of frequency were accessible. For this reason the scaling was conducted using the linear $1/T$ scale, which is isomorphic to the logarithmic frequency scale when thermorheological simplicity holds (Sidebottom, 2005). As shown in Fig. 16, the quantity $\varepsilon''T$ obtained at a series of fixed frequencies could be scaled by appropriate shift along the $1/T$ axis so as to collapse data onto a common curve. The required shift, shown in the inset, indicates an activation energy identical with that observed for the scaling of data at higher temperatures. While the collapse was complete at both high and low temperatures for all samples, the collapse was not successful for the larger cations at intermediate

temperatures. This can be seen in Fig. 16, where the master curve of KPO_3 shows a distinct failure to collapse in the range $4<1000/T<9$. In this way, it was revealed that for the large cation metaphosphate glasses the loss contained a nonionic contribution that could be separated from the ionic portion. This nonionic portion was attributed to the local restricted motions of the nonbridging oxygens in these constricted ion-conducting glasses.

X. SUMMARY

An understanding of ion motion in materials is clearly needed for the continuing development of solid state ionic devices. In so much as it is possible, given the length constraints, we have tried to emphasize how impedance spectroscopy techniques can best be employed to further our collective understanding of these ion-conducting materials. The coverage offered here is by no means a complete canvas of all the literature on the subject, and owing to its narrow focus has left out many important insights gleaned from other experimental techniques. Throughout, we have emphasized the significance of thermal-rheological simplicity and the scaling properties of the ac permittivity arising from ionic motions over earlier analysis schemes (e.g., the electric modulus) that dominated the literature prior to about 1994. In summary, we have endeavored here to describe, through a review of numerous illustrative examples, how experimental measurements of the ac impedance can be analyzed in a direct fashion to obtain significant information regarding the mean-squared displacement of the mobile ions.

REFERENCES

Almond, D. P., G. K. Duncan, and A. R. West, 1983, "The determination of hopping rates and carrier concentrations in ionic conductors by a new analysis of ac conductivity," Solid State Ionics **8**, 159.

Almond, D. P., and A. R. West, 1983a, "Mobile ion concentrations in solid electrolytes from an analysis of ac conductivity," Solid State Ionics **9-10**, 277.

Almond, D. P., and A. R. West, 1983b, "Impedance and modulus spectroscopy of real dispersive conductors," Solid State Ionics **11**, 57.

Almond, D. P., A. R. West, and R. J. Grant, 1982, "Temperature dependence of the ac conductivity of Na β-alumina," Solid State Commun. **44**, 1277.

Anderson, O. L., and D. A. Stuart, 1954, "Calculation of activation energy of ionic conductivity in silica glasses by classical methods," J. Am. Ceram. Soc. **37**, 573.

ASTM designation D150-94, 1995, Am. Soc. for Testing and Materials, Annual book of ASTM standards.

Bernasconi, J., H. U. Beyler, and S. Strassler, 1979, "Anomalous frequency-dependent conductivity in disordered one-dimensional systems," Phys. Rev. Lett. **42**, 819.

Bunde, A., M. D. Ingram, P. Maass, and K. L. Ngai, 1991, "Diffusion with memory: A model for mixed alkali effects in vitreous ionic conductors," J. Phys. A **24**, L881.

Cramer, C., K. Funke, T. Saatkamp, D. Wilmer, and M. D. Ingram, 1995, "High-frequency conductivity plateau and ionic hopping processes in a ternary lithium borate glass," Z. Naturforsch., A: Phys. Sci. **50a**, 613.

Day, D. E., 1976, "Mixed alkali glasses: Their properties and uses," J. Non-Cryst. Solids **21**, 343.

Dyre, J. C., 1986, "Mechanism of glass ionic conductivity," J. Non-Cryst. Solids **88**, 271.

Dyre, J. C., 1993, "Universal low-temperature ac conductivity of macroscopically disordered nonmetals," Phys. Rev. B **48**, 12511

Dyre, J. C., and T. B. Schroder, 2000, "Universality of ac conduction in disordered solids," Rev. Mod. Phys. **72**, 873.

Elliott, S. R., 1994a, "Frequency-dependent conductivity in ionically and electronically conducting amorphous solids," Solid State Ionics **70-71**, 27.

Elliott, S. R., 1994b, "Use of the modulus formalism in the analysis of ac conductivity data for ionic glasses," J. Non-Cryst. Solids **170**, 97.

Funke, K., 1993, "Jump relaxation in solid electrolytes," Prog. Solid State Chem. **22**, 111.

Funke, K., and D. Wilmer, 1999, "Concept of mismatch and relaxation derived from conductivity spectra of solid electrolytes," Mater. Res. Soc. Symp. Proc. **548**, 403.

Gefen, Y., A. Aharony, and S. Alexander, 1983, "Anomalous diffusion on percolating clusters," Phys. Rev. Lett. **50**, 77.

Greaves, G. N., 1989, "EXAFS, glass structure and diffusion," Philos. Mag. B **60**, 793.

Greaves, G. N., S. J. Gurman, C. R. A. Catlow, A. V. Chadwick, S. Houde-Walter, C. M. B. Henderson, and B. R. Dobson, 1991, "A structural basis for ionic diffusion in oxide glasses," Philos. Mag. A **64**, 1059.

Hodge, I. M., K. L. Ngai, and C. T. Moynihan, 2005, "Comments on the electric modulus function," J. Non-Cryst. Solids **351**, 104.

Howell, F. S., R. A. Bose, P. B. Macedo, and C. T. Moynihan, 1974, "Electrical relaxation in a glass-forming molten salt," J. Phys. Chem. **78**, 639.

Huang, W. C., and H. Jain, 1995, "Correlation between local structure and electrical response of Rb and (Rb, Ag) germanate glasses: dc conductivity," J. Non-Cryst. Solids **188**, 254.

Hyde, J. M., M. Tomozawa, and M. Yoshiyagawa, 1987, "A comparison of the dielectric characteristics of single alkali and mixed alkali glasses," Phys. Chem. Glasses **28**, 174.

Ingram, M. D., 1994, "The mixed alkali effect revisited: A new look at an old problem," Glass Sci. Technol. (Offenbach, Ger.) **67**, 151.

Iwauchi, K., and Y. Ikeda, 1992, "Dielectric properties of monoclinic hollandite $Ba_xTi_{4-2x}Fe_{2x}O_8$," Phys. Status Solidi A **130**, 449.

Jackson, J. D., 1975, *Classical Electrodynamics*, 2nd ed. (Wiley, New York).

Jain, H., 1993, in *Experimental Techniques of Glass Science*, edited by C. J. Simmons and O. H. El-Bayoumi (American Ceramic Society, Westerville, OH), p. 433.

Jain, H., E. I. Kamitsos, Y. D. Yiannopoulos, G. D. Chryssikos, W. C. Huang, R. Kuchler, and O. Kannert, 1996, "A comprehensive view of the local structure around Rb in rubidium germanate glasses," J. Non-Cryst. Solids **203**, 320.

Jonscher, A. K., 1977, "The universal dielectric response," Nature (London) **267**, 673.

Jonscher, A. K., 1983, *Dielectric Relaxation in Solids* (Chelsea Dielectrics, London).

Jund, P., W. Kob, and R. Jullien, 2001, "Channel diffusion of sodium in a silicate glass," Phys. Rev. B **64**, 134303.
Kahnt, H., 1991, "Ionic transport in oxide glasses and frequency dependence of conductivity," Ber. Bunsenges. Phys. Chem. **95**, 1021.
Kanert, O., R. Kuchler, J. Dieckhofer, X. Lu, and H. Jain, 1994, "Correspondence between nuclear-spin relaxation and electrical conductivity in glasses at low temperatures," Phys. Rev. B **49**, 629.
Kanert, O., R. Kuchler, K. L. Ngai, and H. Jain, 1994, "Significant differences between nuclear-spin relaxation and conductivity relaxation in low-conductivity glasses," Phys. Rev. B **49**, 76.
Kittel, C., 2005, *Introduction to Solid State Physics*, 8th ed. (Wiley, New York).
Krogh-Moe, J., 1965, "Interpretation of the infrared spectra of boron oxide and alkali borate glasses," Phys. Chem. Glasses **6**, 46.
Kubo, R., 1957, "Statistical-mechanical theory of irreversible processes. I. General theory and simple applications to magnetic and conduction problems," J. Phys. Soc. Jpn. **12**, 570.
Kudo, T., and K. Fueki, 1990, *Solid State Ionics* (VCH, Weinheim, Germany).
Lu, X., and H. Jain, 1994, "Low temperature ac conductivity of oxide glasses," J. Phys. Chem. Solids **55**, 1433.
Maass, P., A. Bunde, and M. D. Ingram, 1992, "Ion transport anomalies in glasses," Phys. Rev. Lett. **68**, 3064.
Macdonald, J. R., 1994, "Power-law exponents and hidden bulk relaxation in the impedance spectroscopy of solids," J. Electroanal. Chem. **378**, 17.
Macdonald, J. R., 2005, "Universality, the Barton Nakajima Namikawa relation, and scaling for dispersive ionic materials," Phys. Rev. B **71**, 184307.
Macdonald, J. R., 2007, "Dynamics of mobile ions: Fitting of CKN frequency response data without an excess wing," J. Phys. Chem. B **111**, 7064.
Macedo, P. B., C. T. Moynihan, and R. Bose, 1972, "The role of ionic diffusion in polarization in vitreous ionic conductors," Phys. Chem. Glasses **13**, 171.
McCrum, N. G., B. E. Read, and G. Williams, 1967, *Anelastic and Dielectric Effects in Polymeric Solids* (Wiley, New York).
Moynihan, C. T., 1994, "Analysis of electrical relaxation in glasses and melts with large concentrations of mobile ions," J. Non-Cryst. Solids **172-174**, 1395.
Moynihan, C. T., L. P. Boesch, and N. L. Laberge, 1973, "Decay function for the electric field relaxation in vitreous ionic conductors," Phys. Chem. Glasses **14**, 122.
Murugavel, S., and B. Roling, 2002, "ac conductivity spectra of alkali tellurite glasses: Composition-dependent deviations from the Summerfield scaling," Phys. Rev. Lett. **89**, 195902.
Murugavel, S., and B. Roling, 2003, "Nearly constant dielectric loss of glasses containing different mobile alkali ions," J. Non-Cryst. Solids **330**, 122.
Ngai, K. L., 1979, "Universality of low-frequency fluctuation, dissipation and relaxation properties of condensed matter," Comments Solid State Phys. **9**, 127.
Ngai, K. L., 1999, "Properties of the constant loss in ionically conducting glasses, melts, and crystals," J. Chem. Phys. **110**, 10576.
Ngai, K. L., G. N. Greaves, and C. T. Moynihan, 1998, "Correlation between the activation energies for ionic conductivity for short and long time scales and the Kohlrausch stretching parameter β for ionically conducting solids and melts," Phys. Rev. Lett. **80**, 1018.
Ngai, K. L., and O. Kanert, 1992, "Comparisons between the coupling model predictions, Monte Carlo simulations and some recent experimental data of conductivity relaxations in glassy ionics," Solid State Ionics **53-56**, 936.
Ngai, K. L., and C. Leon, 1999, "Relating macroscopic electrical relaxation to microscopic movements of the ions in ionically conducting materials by theory and experiment," Phys. Rev. B **60**, 9396.
Ngai, K. L., and S. W. Martin, 1989, "Correlation between the activation enthalpy and Kohlrausch exponent for ionic conductivity in oxide glasses," Phys. Rev. B **40**, 10550.
Ngai, K. L., and C. T. Moynihan, 1998, "The dynamics of mobile ions in ionically conducting glasses and other materials," MRS Bull. **23** (11), 51.
Ngai, K. L., J. N. Mundy, H. Jain, O. Kanert, and G. Balzer-Jollenbeck, 1989, "Correlation between the activation enthalpy and Kohlrausch exponent for ionic conductivity in alkali aluminogermanate glasses," Phys. Rev. B **39**, 6169.
Ngai, K. L., and R. W. Rendell, 1991, "Toward a theory of relaxation in correlated systems: Diffusion in the phase space of a chaotic Hamiltonian," J. Non-Cryst. Solids **131-133**, 233.
Nowick, A. S., and B. S. Lim, 1994, "Analysis of ac conductivity for Na_2O-3SiO_2 glass by stretched exponential and Jonscher power-law methods," J. Non-Cryst. Solids **172-174**, 1389.
Nowick, A. S., A. V. Vaysleyb, and W. Liu, 1998, "Identification of distinctive regimes of behavior in the ac electrical response of glasses," Solid State Ionics **105**, 121.
Patel, H. K., 1993, Ph.D. thesis (Iowa State University, Ames, IA).
Patel, H. K., and S. W. Martin, 1992a, "Fast ionic conduction in $Na_2S+B_2S_3$ glasses: Compositional contributions to nonexponentiality in conductivity relaxations," Solid State Ionics **53-56**, 1148.
Patel, H. K., and S. W. Martin, 1992b, "Fast ionic conduction in $Na_2S+B_2S_3$ glasses: Compositional contributions to nonexponentiality in conductivity relaxation in the extreme low-alkali-metal limit," Phys. Rev. B **45**, 10292.
Pimenov, A., P. Lunkenheimer, H. Rall, R. Kohlhaas, and A. Loidl, 1996, "Ion transport in the fragile glass former 3KNO_3-2$Ca(NO_3)_2$," Phys. Rev. E **54**, 676.
Provenzano, V., L. P. Boesch, V. Volterra, C. T. Moynihan, and P. B. Macedo, 1972, "Electrical relaxation in Na_2O3SiO_2 glass," J. Am. Ceram. Soc. **55**, 492.
Rivera, A., C. Leon, C. P. E. Varsamis, G. D. Chryssikos, K. L. Ngai, C. M. Roland, and L. J. Buckley, 2002, "Cation mass dependence of the nearly constant dielectric loss in alkali triborate glasses," Phys. Rev. Lett. **88**, 125902.
Roling, B., 1998, "Scaling properties of the conductivity spectra of glasses and supercooled melts," Solid State Ionics **105**, 185.
Roling, B., 1999, "What do electrical conductivity and electrical modulus spectra tell us about the mechanisms of ion transport processes in melts, glasses, and crystals?," J. Non-Cryst. Solids **244**, 34.
Roling, B., and C. Martiny, 2000, "Nonuniversal features of the ac conductivity in ion conducting glasses," Phys. Rev. Lett. **85**, 1274.
Roling, B., C. Martiny, and S. Bruckner, 2001, "Ion transport in glass: Influence of glassy structure on spatial extent of nonrandom ion hopping," Phys. Rev. B **63**, 214203.
Roling, B., C. Martiny, and K. Funke, 1999, "Information on

the absolute length scales of ion transport processes in glasses from electrical conductivity and tracer diffusion data," J. Non-Cryst. Solids **249**, 201.
Scher, H., and M. Lax, 1973a, "Stochastic transport in a disordered solid. I. Theory," Phys. Rev. B **7**, 4491.
Scher, H., and M. Lax, 1973b, "Stochastic transport in a disordered solid. II. Impurity conduction," Phys. Rev. B **7**, 4502.
Schroder, T. B., and J. C. Dyre, 2000, "Scaling and universality of ac conduction in disordered solids," Phys. Rev. Lett. **84**, 310.
Shelby, J. E., 1983, "Thermal expansion of alkali borate glasses," J. Am. Ceram. Soc. **66**, 225.
Sidebottom, D. L., 1999a, "A universal approach for scaling the a. c. conductivity in ionic glasses," Phys. Rev. Lett. **82**, 3653.
Sidebottom, D. L., 1999b, "Ionic conductivity in glasses: Is the window effect statistically relevant?," J. Non-Cryst. Solids **244**, 223.
Sidebottom, D. L., 1999c, "Evidence for site memory effects in the ionic relaxation of $(Li_2O)_x(Na_2O)_y(GeO_2)_{1-x-y}$ glasses," J. Non-Cryst. Solids **255**, 67.
Sidebottom, D. L., 1999d, "Dimensionality dependence of the conductivity dispersion in ionic materials," Phys. Rev. Lett. **83**, 983.
Sidebottom, D. L., 2000, "Influence of cation constriction on the ac conductivity dispersion in metaphosphate glasses," Phys. Rev. B **61**, 14507.
Sidebottom, D. L., 2005, "Constriction effect in the nearly constant loss of alkali metaphosphate glasses," Phys. Rev. B **71**, 134206.
Sidebottom, D. L., P. F. Green, and R. K. Brow, 1995a, "Comparison of KWW and power law analyses of an ion-conducting glass," J. Non-Cryst. Solids **183**, 151.
Sidebottom, D. L., P. F. Green, and R. K. Brow, 1995b, "Two contributions to the ac conductivity of alkali oxide glasses," Phys. Rev. Lett. **74**, 5068.
Sidebottom, D. L., P. F. Green, and R. K. Brow, 1995c, "Anomalous diffusion model of ionic transport in oxide glasses," Phys. Rev. B **51**, 2770.
Sidebottom, D. L., and C. M. Murray-Krezan, 2002, "Distinguishing two contributions to the nearly constant loss in ion-conducting glasses," Phys. Rev. Lett. **89**, 195901.
Sidebottom, D. L., B. Roling, and K. Funke, 2000, "Ionic conduction in solids: Comparing conductivity and modulus representations with regard to scaling properties," Phys. Rev. B **63**, 024301.
Sidebottom, D. L., and J. Zhang, 2000, "Scaling of the ac permittivity in ion-conducting glasses," Phys. Rev. B **62**, 5503.
Svare, I., F. Borsa, D. R. Torgeson, and S. W. Martin, 1993, "Correlation functions for ionic motion from NMR relaxation and electrical conductivity in the glassy fast-ion conductor $(Li_2S)_{0.56}(SiS_2)_{0.44}$," Phys. Rev. B **48**, 9336.
Tipler, P. S., 1999, *Physics for Scientists and Engineers*, 4th ed. (Freeman and Worth, New York).
Tomozawa, M., 1977, in *Treatise on Materials Science*, edited by M. Tomozawa (Academic, New York), Vol. 12, p. 283.